

Journal of Materials Chemistry C

Accepted Manuscript



This is an *Accepted Manuscript*, which has been through the Royal Society of Chemistry peer review process and has been accepted for publication.

Accepted Manuscripts are published online shortly after acceptance, before technical editing, formatting and proof reading. Using this free service, authors can make their results available to the community, in citable form, before we publish the edited article. We will replace this *Accepted Manuscript* with the edited and formatted *Advance Article* as soon as it is available.

You can find more information about *Accepted Manuscripts* in the [Information for Authors](#).

Please note that technical editing may introduce minor changes to the text and/or graphics, which may alter content. The journal's standard [Terms & Conditions](#) and the [Ethical guidelines](#) still apply. In no event shall the Royal Society of Chemistry be held responsible for any errors or omissions in this *Accepted Manuscript* or any consequences arising from the use of any information it contains.



Water stability and orthogonal patterning of flexible micro-electrochemical transistors on plastic

Shiming Zhang¹, Elizabeth Hubis¹, Camille Girard¹, Prajwal Kumar¹, John DeFranco² and Fabio Cicoira^{1,a}

Received 00th January 20xx,
Accepted 00th January 20xx

DOI: 10.1039/x0xx00000x

www.rsc.org/

Water-stable, flexible and micro-scale organic electrochemical transistors (OECTs) based on poly(3,4-ethylenedioxythiophene) doped with poly(styrenesulfonate) (PEDOT:PSS) were fabricated on a plastic substrate using a new process based on a fluorinated photoresist. The PEDOT:PSS films, mixed solely with a biocompatible conductivity enhancer, show robust adhesion on plastic substrates, and exhibit unchanged electrical properties under extreme bending. This work simplifies the fabrication of high-performance OECTs and places them in a highly competitive position for flexible electronics and healthcare applications.

Introduction

Organic electronic devices present unique advantages with respect to their inorganic counterparts, such as low temperature processing, possibility to tune electronic properties via chemical synthesis, mixed electronic/ionic conduction and compatibility with printing and patterning techniques on flexible and lightweight substrates^{1,2}. In recent years, research on organic conducting polymer devices, such as organic electrochemical transistors (OECTs) and microelectrodes, has gained great momentum for applications in bioelectronics^{3,4}. OECTs, being able to directly interface with aqueous electrolytes, can sense chemical and biological signals originating from redox processes⁵. OECTs based on poly(3,4-ethylenedioxythiophene) doped with poly(styrenesulfonate) (PEDOT:PSS) have already been used to detect biologically relevant species, such as glucose⁶, neurotransmitters⁷ and

DNA⁸, to monitor tissue integrity⁹, and to record brain activity or local-field potentials in vivo^{10,11}. Organic electronic ion pumps based on OECTs have been used as implantable devices for in vivo treatment of neuropathic pain¹².

The development of organic bioelectronics calls for viable processes to fabricate miniaturized devices on flexible substrates with long-term stability in aqueous media. Miniaturized OECT arrays are highly desired, e.g. to study the activity of individual brain cells, whose typical size ranges between 1 and 20 μm ^{13,14}. Flexible and conformable substrates allow to effectively place devices in contact with curvilinear and non-uniform surfaces often encountered in biomedical applications¹¹. Long-term stability (i.e. no delamination) of conducting polymer films in aqueous media is essential for bioelectronics, where applications such as implantable electrodes for chronic recording and stimulation are envisaged¹⁵. To date, a great deal of work has been dedicated to the development of flexible OECTs and electrodes¹⁶⁻¹⁸. Berggren et al. have reported lithographic patterning of commercially available PEDOT:PSS coated plastic sheets (Agfa Orgacon EL-350) with a lateral resolution above 100 μm .¹⁹ However, the production of PEDOT:PSS coated plastic sheets has been

¹Department of Chemical Engineering, Polytechnique Montréal, Montréal, Québec, H3C3J7, Canada

²Orthogonal, Inc., 1999 Lake Avenue, Rochester, NY 14650, U.S.A.

^a Author to whom correspondence should be addressed. Electronic mail:

Fabio.cicoira@polymtl.ca

Electronic Supplementary Information (ESI) available: [details of any supplementary information available should be included here]. See DOI: 10.1039/x0xx00000x

recently discontinued by Agfa. Malliaras et al. have recently reported OECTs on ultrathin Parylene C films for measurements of in-vivo brain activity²⁰. However, the long-term stability of OECTs in aqueous media has not been deeply investigated so far. Moreover, high-throughput and environmentally friendly fabrication processes of miniaturized conducting polymer devices are highly demanded.

In this work we fabricated micro-scale OECTs, based on PEDOT:PSS, on flexible plastic substrates. Our PEDOT:PSS films show robust adhesion on plastic, long-term stability in aqueous media and no significant changes of their electrical properties under extreme bending. OECT patterning was achieved with a photolithographic process making use of photoresists, developers and strippers based on fluorinated materials. These materials are “orthogonal” to both polar and nonpolar solvents and, as such, are completely non-interacting with PEDOT:PSS films, which therefore are not damaged during the patterning process^{21,22}. Our OECTs can be operated at low voltage (below 1V) and exhibit stable electrical characteristics after multiple reduction/oxidation voltammetric cycles. Our results studies are of paramount importance for the development of flexible and stable OECTs aiming at biological and healthcare applications.

Results and Discussion

The process we employed to fabricate flexible OECTs is illustrated in Fig.1 (see detailed procedure in ESI). Pre-cleaned polyethylene terephthalate (PET) sheets (thickness of about 180 μm) were laminated on a glass wafer pre-covered with a Polydimethylsiloxane (PDMS) layer, to ensure flatness and rigidity during the lithography steps. Au source/drain contacts (40 nm thickness with 4 nm Cr as adhesion layer), with distances ranging from 100 μm to 5 μm , were patterned by conventional photolithography, metal deposition and lift-off. The Au-patterned PET substrates were treated by UV-ozone before PEDOT:PSS film deposition. PEDOT:PSS films were deposited by spin coating from mixtures containing a PEDOT:PSS aqueous suspension (CleviosTM PH1000, Heraeus), the conductivity enhancer glycerol and occasionally dodecylbenzenesulfonic (DBSA) acid and 3-glycidoxypropyltrimethoxysilane (GOPS). After spin coating, the films were dried on a hotplate at 100 $^{\circ}\text{C}$ for 20 min. PEDOT:PSS

OECT channels were patterned using a subtractive process consisting of sequential film deposition, photolithography and etching. A negative-tone fluorinated photoresist (OSCoR 4000, Orthogonal, Inc.) was spin-coated on the PEDOT:PSS film, baked on a hotplate (and exposed to the UV light of the mask aligner through a photomask). After a post-exposure baking, the unexposed photoresist was developed using a puddle method. The unprotected PEDOT:PSS was then etched by oxygen reactive ion etching (RIE) and the exposed photoresist remaining on the patterned PEDOT:PSS film was removed by immersing the samples in a fluorinated stripper. A further photolithography step was performed to cover the Au electrodes with photoresist in order to prevent their direct contact with the electrolyte. At the end of the fabrication process, the devices were soaked in deionized water to remove saline contaminants from the PEDOT:PSS film. This procedures yielded transistors featuring channel lengths (L) ranging from 5 μm to 100 μm and widths (W) of 80 μm and 400 μm . Finally, a glass or PDMS well was attached on the channel area to confine the electrolyte. A high surface area (1000–2000 m^2g^{-1}) activated carbon was used as the gate electrode.

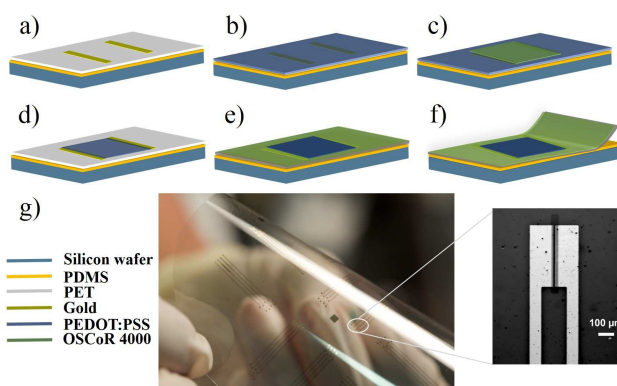


Fig.1. Scheme of the fabrication processes of flexible OECTs: a) photolithography patterning of gold electrodes on PET sheets laminated on PDMS/glass; b) PEDOT:PSS spin-coating; c) spin coating and photolithographic patterning of the fluorinated photoresist on PEDOT:PSS; d) oxygen reactive ion etching of PEDOT:PSS and photoresist removal; e) second photoresist pattern to protect the metal electrodes; f) detachment of PET from PDMS/glass; g) digital photograph of devices on a flexible PET foil and optical microscopy image showing the Au electrodes and the patterned PEDOT:PSS channel (the channel length/width is 5 μm /400 μm , the dark area between the two Au electrodes corresponds to the patterned PEDOT:PSS channel).

The long term stability of PEDOT:PSS films on PET in aqueous media was benchmarked with respect to analogous films deposited on glass. Three different formulations were used for the spin coating mixtures, i.e. PEDOT:PSS/glycerol,

PEDOT:PSS/DBSA and PEDOT:PSS/glycerol/DBSA/GOPS. While glycerol acts as a conductivity enhancer, DBSA is used to facilitate film processing and GOPS as a crosslinker to improve film stability on glass substrates^{20, 23, 24}. The effect of additives (DBSA and GOPS) has been studied for PEDOT:PSS films deposited on glass, but it is still unknown for films deposited plastic substrates. We found that films on glass delaminated within 1 day after water immersion unless GOPS was introduced, as previously reported²³, whereas films on plastic did not delaminate even in absence of GOPS.

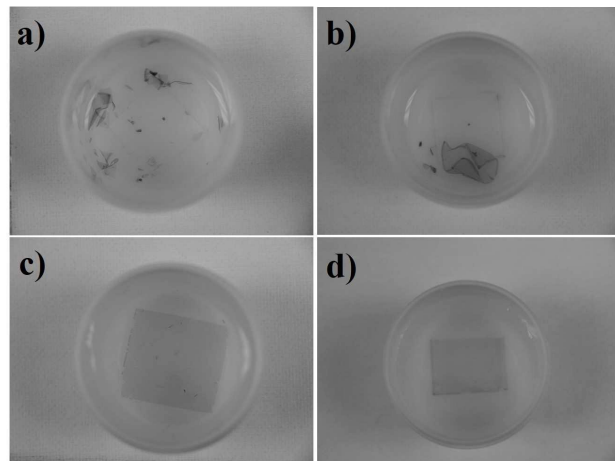


Fig.2. PEDOT:PSS films on glass and PET substrates after solvent immersion. a) PEDOT:PSS/5 v/v. % glycerol/0.5 v/v. % DBSA on glass after 1 day in DI water; b) PEDOT:PSS/5 v/v. % glycerol/0.5 v/v. % DBSA/1 v/v. % GOPS on glass after 1 day of immersion in water, whereas those containing GOPS delaminate after about 3-month. Films on PET containing only PEDOT:PSS and glycerol do not delaminate even after 3-month in DI water or PBS.

Remarkably, PEDOT:PSS films on PET did not detach from the substrate even after 3 month in water (Fig.2) while films on glass with GOPS showed detachment after 3 months water immersion. Similar results were achieved upon immersion into phosphate buffered saline (PBS). These results prove that the crosslinking agent GOPS is not indispensable for PEDOT:PSS film on PET. This is an important point since GOPS has the drawback to significantly decrease the electronic and ionic conductivity of PEDOT:PSS films^{23, 25}. We also observed good film quality without DBSA, although it facilitates film processing and improves film conductivity on glass substrate²³. Film obtained from mixtures containing PEDOT:PSS and

glycerol showed electrical conductivities as high as ~ 600 S/cm, similar to those obtained on glass in the absence of GOPS²³. Immersion of these films in aqueous media led to a thickness decrease accompanied by a sheet resistance increase (see ESI), likely due to the removal of PSS from the film surface²³. However these changes did not significantly affect the film conductivity. Overall, these findings point to an enhanced water stability of PEDOT:PSS on plastic substrates with respect to films on glass.

To gain insight into the flexibility of our PEDOT:PSS films, we measured the change of the current flowing through them upon increasing substrate bending (Fig.3a). For this measurements we used ~ 70 nm PEDOT:PSS films deposited on PET sheets with electrodes made by copper tape covered by silver paste. The current did not show any significant decrease upon increasing substrate bending (Fig.3a): a current loss of about 1% was observed when bending the film from 0 to 100% for the first 100 bending cycles (see Fig.3 for the definition of bending percentage). After 500 bending cycles, the current loss was less than 4%, which demonstrates a good bendability of the films, in line with recent reports on flexible OEECTs¹⁷. These results prove that PEDOT:PSS containing only the conductivity enhancer glycerol are excellent candidates for flexible devices on PET.

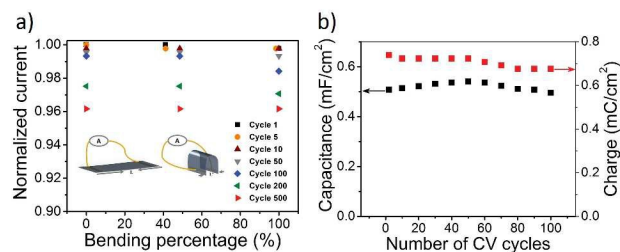


Fig.3. a) Normalized current versus film bending. The inset shows the schematic of bending test methods of the PEDOT:PSS films on PET. The bending percentage is defined as $[(L-L')/L] \times 100\%$. b) Capacitance (left axis) and anodic charge (right axis) extracted from CV of films processed from PEDOT:PSS and 5 v/v. % glycerol.

We subsequently studied the redox voltammetric stability of PEDOT:PSS films (with 5 v/v. % glycerol) on PET using cyclic voltammetry (CV). The amount of electrical charge Q (C) accumulated in the PEDOT:PSS film during doping for each 10 cycles was calculated by integrating the anodic current over time. Similarly the pseudocapacitance was calculated from

the slope of the integrated charge (during doping) vs. electrode potential for every 10 cycles. Our results (Fig.3b) show that stable charges and capacitances were maintained for up to 100 scan cycles, which indicates a good redox stability of PEDOT:PSS films on plastic.

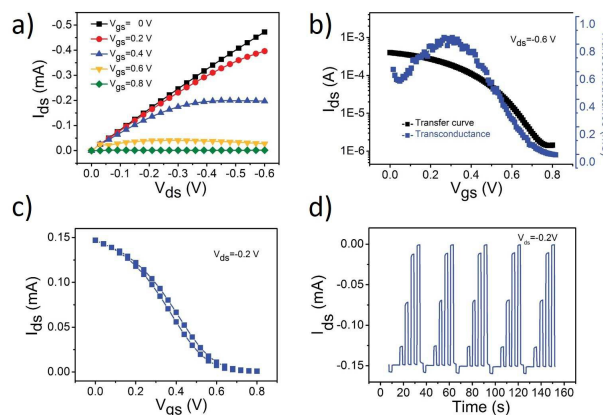


Fig.4. Electrical characteristics of OECT on PET. (a) Output characteristics with V_{ds} swept from 0 V to -0.6 V and V_{gs} varying from 0 (top curve) to 0.8 V (bottom curve) with a step of 0.2 V. (b) Transfer curve for $V_{ds} = -0.6$ V and V_{gs} sweeping from 0 to 0.8 V and the associated transconductance. (c) Hysteresis curve for V_{gs} varying from 0 to 0.8 V at $V_{ds} = -0.2$ V with sweeping rate of 200 mV/s. (d) Transient characteristics (I_{ds} versus time) measured at a fixed drain-source voltage (V_{ds}) while pulsing for 2 seconds the gate-source voltage (V_{gs}) from from -0.2 to 0.8 V in 0.2 V steps.

Finally, we characterized micro-OECTs on PET (channel width 80 μm and channel length 5 μm) employing a 0.01M aqueous NaCl solution as the electrolyte and a high surface area activated carbon (AC) as the gate electrode. AC gate electrodes lead to large current modulations and do not require any additional reference electrode to monitor the channel potential due to their high double-layer capacitance²⁶. Fig.4 (a) and (b) show the output and transfer characteristics of the OECTs. The transistor shows linear output curves at $V_{gs} = 0$, in agreement with the high conductivity of PEDOT:PSS. Saturation behaviour appears at a gate bias ranging from 0.2 V to 0.8 V. An ON/OFF ratio of about 300 and a maximum transconductance of about 0.8 mS is extracted for the device with 5 μm length and 80 μm width at $V_{ds} = -0.6$ V from the transfer plot in Fig.4b. The transconductance is comparable with results (~0.1 mS -1 mS) obtained on glass substrates^{16, 27}. This transconductance can be further improved by increasing the film thickness (only ~70 nm used in this work) since a higher film thickness leads to higher transconductance²⁷. In addition, our devices show minor hysteresis (Fig.4c) between 0

V and 0.8 V gate voltage, similarly to our recent studies on glass substrates.²⁸ These results indicate a relatively fast dedoping/doping of the PEDOT:PSS films on PET substrates by electrolyte ions due to the small film volume. Fig.4d shows that for transient OECT measurements the current at gate voltages ranging from -0.2 V to 0.8 V remains stable for successive cyclic measurements. We also measured the mobility of our patterned PEDOT:PSS film on PET⁵, and extracted a value of ca. $10^{-1} \text{ cm}^2 \text{ V}^{-1} \text{ S}^{-1}$ (see ESI), which is similar to results on glass substrates.

Conclusions

In summary, we have demonstrated stable OECTs based on PEDOT:PSS on plastic substrates. PEDOT:PSS films, processed from a mixture containing only PEDOT:PSS and glycerol, remain stable even after 3 months of immersion in water and PBS, which demonstrates a robust film adhesion on plastic. Bending tests show that the films can undergo extreme bending with negligible effect on the current. Flexible OECTs arrays with channel lengths as short as 5 μm were achieved by directly patterning PEDOT:PSS films on PET with a fluorinated photoresist. OECT characterization further proves that the devices have good performance on plastic. Our results contribute to overcome some of the challenges faced when developing large-scale processing of flexible and stable devices.

Acknowledgments

The authors are grateful to Clara Santato and Gaia Tomasello for fruitful discussions and Daniel Pilon for technical support. This work is supported by grants Discovery (NSERC) and *Établissement de Nouveau Chercheur* (FRQNT) awarded to F.C. S.Z. is grateful to NSERC for financial support through a Vanier Canada Graduate Scholarship. C.G. is grateful to NSERC for financial support through an Undergraduate Student Research Award. The authors are grateful to CMC Microsystems for financial support through the programs MNT financial assistance and CMC Solutions. We have also benefited from the support of FRQNT and its *Regroupement stratégique* program through a grant awarded to RQMP.

Materials and Methods

Polyethylene terephthalate (PET) sheets were purchased from Policrom Inc (Bensalem, PA, USA). The PEDOT:PSS aqueous suspension (Clevios™ PH1000) was purchased from Heraeus Electronic Materials GmbH (Leverkusen, Germany). Glycerol (99.5+ % purity) was purchased from Caledon Laboratories Ltd (Georgetown, ON). Dodecylbenzenesulfonic acid (DBSA, 95+% purity) and anhydrous 3-glycidioxypropyltrimethoxysilane (GOPS, 98+% purity) were obtained from Sigma-Aldrich Canada Ltd. (Oakville, ON). The Fluorinated photoresist kit, including a negative-tone chemically amplified photoresist (OSCoR 4000), a developer and a stripper, was supplied by Orthogonal Inc. (Rochester, NY, USA). A Karl Suss MA-6/BA-6 mask aligner (wavelength 365 nm, intensity of ~8 mW/cm²) was used for photolithography. Reactive ion etching was performed with an ENI OEM-6 apparatus. Cyclic voltammetry measured was performed with BioLogic Science Instruments VSP-300. Transistor characterization and electrical measurements under bending were performed using an Agilent B2902A source-measure unit controlled by Labview software. The film thickness was measured with a profilometer (Dektak 150) and the sheet resistance was obtained by four point probe measurements.

References

1. S. R. Forrest, *Nature*, 2004, **428**, 911-918.
2. F. Cicoira and C. Santato, *Organic electronics: emerging concepts and technologies*, John Wiley & Sons, 2013.
3. J. Rivnay, R. M. Owens and G. G. Malliaras, *Chemistry of Materials*, 2014, **26**, 679-685.
4. M. Berggren and A. Richter - Dahlfors, *Advanced Materials*, 2007, **19**, 3201-3213.
5. D. A. Bernards and G. G. Malliaras, *Advanced Functional Materials*, 2007, **17**, 3538-3544.
6. S. Y. Yang, F. Cicoira, R. Byrne, F. Benito-Lopez, D. Diamond, R. M. Owens and G. G. Malliaras, *Chemical Communications*, 2010, **46**, 7972-7974.
7. H. Tang, P. Lin, H. L. W. Chan and F. Yan, *Biosensors and Bioelectronics*, 2011, **26**, 4559-4563.
8. P. Lin, X. Luo, I. Hsing and F. Yan, *Advanced Materials*, 2011, **23**, 4035-4040.
9. L. H. Jimison, S. A. Tria, D. Khodagholy, M. Gurfinkel, E. Lanzarini, A. Hama, G. G. Malliaras and R. M. Owens, *Advanced Materials*, 2012, **24**, 5919-5923.
10. D. Khodagholy, T. Doublet, P. Quilichini, M. Gurfinkel, P. Leleux, A. Ghestem, E. Ismailova, T. Hervé, S. Sanaur and C. Bernard, *Nature communications*, 2013, **4**, 1575.
11. D. Khodagholy, J. N. Gelinias, T. Thesen, W. Doyle, O. Devinsky, G. G. Malliaras and G. Buzsáki, *Nature neuroscience*, 2015, **18**, 310-315.
12. A. Jonsson, Z. Song, D. Nilsson, B. A. Meyerson, D. T. Simon, B. Linderöth and M. Berggren, *Science Advances*, 2015, **1**, e1500039.
13. D. Khodagholy, M. Gurfinkel, E. Stavrinidou, P. Leleux, T. Herve, S. Sanaur and G. G. Malliaras, *Applied Physics Letters*, 2011, **99**, 163304.
14. P. Fromherz, *Annals of the New York Academy of Sciences*, 2006, **1093**, 143-160.
15. P. Lin and F. Yan, *Advanced materials*, 2012, **24**, 34-51.
16. D. Khodagholy, J. Rivnay, M. Sessolo, M. Gurfinkel, P. Leleux, L. H. Jimison, E. Stavrinidou, T. Herve, S. Sanaur, R. M. Owens and G. G. Malliaras, *Nat Commun*, 2013, **4**.
17. A. Campana, T. Cramer, D. T. Simon, M. Berggren and F. Biscarini, *Advanced Materials*, 2014, **26**, 3874-3878.
18. C. Liao, C. Mak, M. Zhang, H. L. Chan and F. Yan, *Advanced Materials*, 2015, **27**, 676-681.
19. D. Nilsson, M. Chen, T. Kugler, T. Remonen, M. Armgarth and M. Berggren, *Advanced Materials*, 2002, **14**, 51-54.
20. M. Sessolo, D. Khodagholy, J. Rivnay, F. Maddalena, M. Gleyzes, E. Steidl, B. Buisson and G. G. Malliaras, *Advanced Materials*, 2013, **25**, 2135-2139.
21. P. G. Taylor, J.-K. Lee, A. A. Zakhidov, M. Chazichristidi, H. H. Fong, J. A. DeFranco, G. G. Malliaras and C. K. Ober, *Adv. Mater*, 2009, **21**, 2314-2317.
22. S. Ouyang, Y. Xie, D. Wang, D. Zhu, X. Xu, T. Tan, J. DeFranco and H. H. Fong, *Journal of Polymer Science Part B: Polymer Physics*, 2014, **52**, 1221-1226.
23. S. Zhang, P. Kumar, A. S. Nouas, L. Fontaine, H. Tang and F. Cicoira, *APL Materials*, 2015, **3**, 014911.
24. A. Williamson, M. Ferro, P. Leleux, E. Ismailova, A. Kaszas, T. Doublet, P. Quilichini, J. Rivnay, B. Rózsa and G. Katona, *Advanced Materials*, 2015.
25. E. Stavrinidou, P. Leleux, H. Rajaona, D. Khodagholy, J. Rivnay, M. Lindau, S. Sanaur and G. G. Malliaras, *Advanced Materials*, 2013, **25**, 4488-4493.
26. H. Tang, P. Kumar, S. Zhang, Z. Yi, G. D. Crescenzo, C. Santato, F. Soavi and F. Cicoira, *ACS Applied Materials & Interfaces*, 2015, **7**, 969-973.
27. J. Rivnay, P. Leleux, M. Sessolo, D. Khodagholy, T. Hervé, M. Fioocchi and G. G. Malliaras, *Advanced Materials*, 2013, **25**, 7010-7014.
28. P. Kumar, Z. Yi, S. Zhang, A. Sekar, F. Soavi and F. Cicoira, *Applied Physics Letters*, 2015, **107**, 053303.